

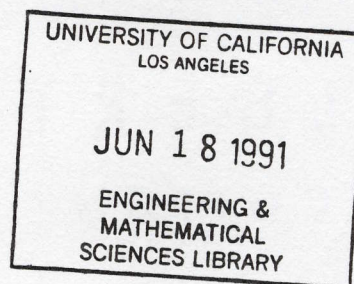
TJ
4
M377B
1990
no. 5

ISSN 1052-6188

Academy of Sciences of the USSR

**JOURNAL OF
MACHINERY
MANUFACTURE
AND RELIABILITY**

*(Problemy mashinostroeniya
i nadezhnosti mashin)*



1990

ALLERTON PRESS, INC.

THE ALLERTON PRESS JOURNAL PROGRAM

in cover-to-cover translation from Russian

JOURNAL OF MACHINERY MANUFACTURE AND RELIABILITY

(Academy of Sciences of the USSR)

(Mashinovedenie)

Editor:	K. V. Frolov	
Assistant Editors:	A. P. Gusenkov G. V. Kreinin V. S. Avduevskii	
Executive Secretary:	N. N. Krasnoshchekov	
Editorial Board:	M. N. Babushkin P. N. Belyanin O. V. Berestnev A. P. Bessonov V. P. Bulatov V. V. Vasil'ev V. A. Vittikh N. A. Generalov F. M. Diment'erg Yu. N. Drozdov S. V. Emel'yanov D. M. Klimov V. V. Klyuev K. S. Kolesnikov A. I. Korendyasev M. V. Korovchinskii A. F. Krainev	N. D. Kiznetsov A. A. Lebedev I. M. Makarov V. A. Mel'nikov V. P. Mishin D. E. Okhotsimskii V. E. Panin S. V. Pinegin V. D. Protasov A. F. Rezchikov M. F. Reshetnev D. N. Reshetov A. F. Selikhov A. P. Semenov V. I. Sergeev G. K. Sorokin

© Izdatel'stvo "Nauka", Mashinovedenie, 1990

© 1990 by Allerton Press, Inc.

Price: \$660.00 (6 issues)

All rights reserved. This publication or parts thereof may not be reproduced in any form without permission of the publisher.

ALLERTON PRESS, INC.
150 Fifth Avenue New York, N.Y. 10011

CONTENTS

NUMBER 5

1990

JOURNAL OF MACHINERY MANUFACTURE AND RELIABILITY

	PAGES	
	RUSSIAN	ENGLISH
The importance of the mechanics of materials and structures in assuring the reliability and safety of engineered systems. V. V. Bolotin	3	1
Precision mechanics based on vibrations and waves. K. M. Ragul'skii and G. P. Kul'vetis	9	6
A procedure for analysis of the dynamics and strength of structures using a damping matrix of general form. E. I. Grigolyuk and N. A. Kulakov	15	12
The recuperative inertia drive as an oscillatory system. I. D. Yudovskii	20	17
Characteristics of a flat bearing with compliant chamber. D. K. Zaitsev and E. G. Grudskaya	26	23
Individual methods for predicting life expectancies of basic power-generating system components. A. A. Chizhik	31	28
Development of methods for evaluation of fatigue-strength characteristics of machine parts. V. P. Kogaev and M. A. Alimov	36	32
A procedure for evaluation of stresses and strains and low-cycle strength of helical-corrugated metal-sleeve shells. A. P. Gusenkov, B. M. Meerson, and G. V. Moskvitin	39	36
Accumulation of fatigue damage in antifriction bearings. O. N. Chermenskii	44	41
Calculation of contact stresses from results of measurements made inside the part. V. I. Kuz'menko	50	46
Fundamental and applied research toward the development of the next generation of equipment for production of hydrogen of special purity using membrane technology. V. M. Makarov	56	51
Modeling the stamping of sheet-metal components by pulsed magnetic field pressure with impact against the block. A. I. Gulidov, V. B. Yudaev, N. V. Kurlaev, and B. A. Bishev	61	55
Operation of a flexible manufacturing system as part of an automated plant. B. I. Cherpakov and V. V. Yukhimov	67	61
Automated subsystems for analysis and synthesis of nonlinear motion-control systems. E. S. Pyatnitskii	74	67
The fracture mechanics of ice and some of its applications. R. V. Gol'dshtein	81	74
Theory of the wear experiment with axisymmetric local contact. M. V. Korovchinskii	89	80

(continued)

THE RECUPERATIVE INERTIA DRIVE AS AN OSCILLATORY SYSTEM

I. D. Yudovskii

Problems of improving the response speeds of cyclic machines by using kinetic-energy accumulators based on mechanisms with nonlinear position functions are discussed. The operating principle is described, the dynamics are analyzed, and the basic characteristics of the system are stated. The properties of the system are compared with those of a traditional self-oscillatory system with elastic elements.

The response speeds and load capacities of cyclic transportation and industrial-transport machines can be increased by using recuperative drives. In recuperation there is a periodic exchange of energy between the final member and an accumulator, and the motor merely compensates kinetic-energy losses. Recuperative-drive cyclic mechanisms are essentially self-oscillatory systems. Thus, recuperative manipulator drives that significantly improved manipulator efficiency have been based on a mass-elasticity oscillatory system [1,2].

At the same time, it is possible to build a recuperative drive using oscillatory systems that do not have potential-energy-accumulating elements. The possibility of such oscillations follows from the equation of motion for conservative systems [3] $a\ddot{q} + 0,5(da/dq)\dot{q}^2 + (d\Pi/dq) = 0$, which admits of periodic solutions at constant potential energy Π if the inertia coefficient a is a periodic function of the generalized coordinate q . Cyclic mechanisms with nonlinear transfer functions possess this property [4]. In these mechanisms, the speed of the driving element is nearly constant, but the periodicity of the transfer function makes the travel of the driving [sic] element nonuniform and is a source of parametric excitation of elastic vibrations in the drive.

For many mechanisms with wide link-speed ranges, interest focuses on periodic motions in which kinetic energy is exchanged between the links of the mechanism and the variations of their potential energy is not a material factor. These mechanisms include inertia-type recuperative drives (Fig. 1) consisting of massive links 1 and 2 joined by a transfer mechanism 3 whose position function is a closed curve without singular points that can be generated, for example, by a jointed-beam four-link [5] (Fig. 1b) or by a variable-ratio belt [6] (Fig. 1c). In position I, shaft O is stationary and shaft O' rotates in the direction indicated by the arrow. On transfer to position II, shaft O accelerates and shaft O' is braked to a stop, etc. Thus, kinetic energy is exchanged between links 1 and 2.

As the massive links move, the transfer function between them varies theoretically from $-\infty$ to $+\infty$ and back with no discontinuities, supporting exchange of kinetic energy between the links at limited accelerations. Automatic variation of the magnitude and sign of the transfer function during motion sets up oscillations of links 1 and 2 with an amplitude determined by the kinematics of the transfer mechanism, with no change in their potential energy. We shall refer to this oscillatory system as an inertia-type kinematic oscillator.

The equation of motion of a system with weightless and nondeformable transfer-mechanism links and ideal couplings in the mechanism has the form

$$(I_1 + I_2 u^2)\ddot{\varphi} + I_2 u u' \dot{\varphi}^2 + M_1 + M_2 u = 0, \quad (1)$$

where I_1 and I_2 are the moments of inertia of links 1 and 2, M_1 and M_2 are the moments of the external forces, reduced to the links; φ , $\dot{\varphi}$, $\ddot{\varphi}$ are the rotation angle, angular velocity, and angular acceleration of link 1, $u = \psi/\dot{\varphi}$ is the transfer function, ψ is the angular velocity of link 2, and $u' = du/d\varphi$.

Since the transfer-mechanism position function of an inertia-type recuperative drive is a closed curve with no breaks, its transfer function on segment $[\Phi_1, \Phi_2]$ (Fig. 2) is continuous and two-valued and consists of decreasing and increasing branches with asymptotes at points Φ_1 and Φ_2 . The branches intersect the φ axes at points P_1 and P_2 . The total amplitude of the oscillations $\Phi = \Phi_1 - \Phi_2$. Let us assume for the sake of argument that the transfer

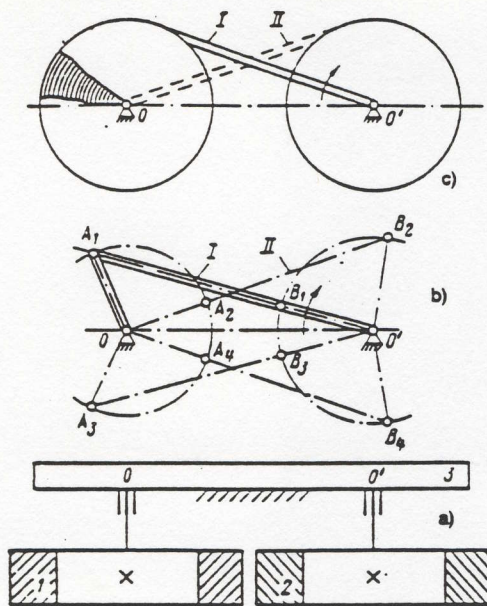


Fig. 1

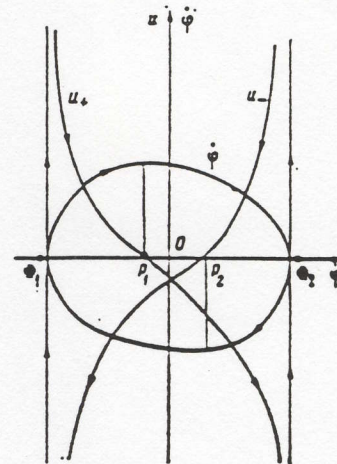


Fig. 2

function specified by the decreasing branch applies as the ϕ coordinate increases, and denote that function by $u_+(\phi)$; the branch that corresponds to motion with a decreasing coordinate will be denoted by $u_-(\phi)$. The directions of variation of the transfer function are indicated by the arrows.

For a conservative system, Eq. (1) can be integrated in quadratures:

$$t_{\pm} = \tau_{\pm} / \dot{\psi}_0, \quad \dot{\phi}_{\pm} = \dot{\psi}_0 \omega_{\pm}, \quad \phi_{\pm} = \dot{\psi}_0^2 \varepsilon_{\pm}, \quad (2)$$

where $\tau_+ = \int_{\phi_1}^{\phi_2} \sqrt{\gamma i_+ + u_+^2} d\phi$, $\tau_- = - \int_{\phi_2}^{\phi_1} \sqrt{\gamma i_- + u_-^2} d\phi$, $\omega_{\pm} = \pm (i_{\pm} + u_{\pm}^2)^{-0.5}$, $\varepsilon_{\pm} = -u_{\pm} u_{\pm}' (i_{\pm} + u_{\pm}^2)^{-2}$,

$i_{\pm} = I_{1\pm} / I_2$, $\dot{\psi}_0 = \sqrt{2E_0 / I_2}$ is the maximum speed of link 2 and corresponds to the total energy E_0 of the system.

In the double indices, the plus sign corresponds to motion of link 1 in the direction of increasing coordinate ϕ , and the minus sign corresponds to its motion in the decreasing direction. The formula for i_{\pm} takes account of the possibility of change in the moment of inertia of link 1 at points ϕ_1 and ϕ_2 , for example on loading and unloading of a manipulator grip.

On the phase diagram, the second equation of (2), being two-valued, specifies a family of phase paths each of which consists of positive and negative branches. Since $u(\phi)$ is continuous on segment $[\phi_1, \phi_2]$ and equal to $\pm \infty$ at its ends, the branches of the phase path have common points $\dot{\phi}(\phi_1) = \dot{\phi}(\phi_2) = 0$, i.e., the phase path is a closed continuous curve and, consequently, describes an oscillatory process. The system's period T is determined by its kinematic (u) and inertial (i) characteristics and depends on the initial conditions $\dot{\psi}_0$: $T = [\tau_+(\phi_2) + \tau_-(\phi_1)] / \dot{\psi}_0$.

Let us illustrate the properties of the above oscillatory systems with reference to mechanisms with transfer functions of the form

$$u_{\pm}(\phi) = \mp (\Phi_0^2 \phi^{-2} - 1)^{-0.5}. \quad (3)$$

This type of function (Fig. 3a) is generated in a variable-ratio belt system with a belt of constant thickness and strong variation of the roll radii, in a hinged four-link in which the distance between centers is much greater than the lengths of the beams and the angle ϕ_0 is small, in an ellipsograph between its slides, and in other mechanisms.

The period of the system's oscillations can be expressed in terms of a complete elliptic integral of the second kind

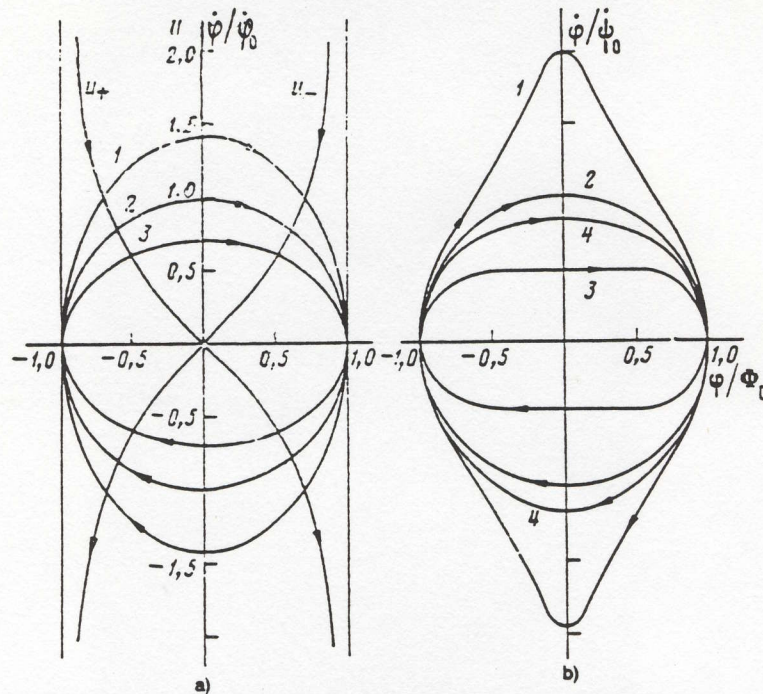


Fig. 3. 1) 1 = 4, 2) 1, 3) 0.25, 4) displacement of load from points $\Phi_1 = \Phi_0$ in points $\Phi_2 = \Phi_0$ when $I_{1+} = 1.4$ and $I_{1-} = 0.7 I_2$.

$$T = \begin{cases} 4\Phi_0\dot{\varphi}_0^{-1}E\left(\frac{\pi}{2}, \sqrt{1-i}\right) & \text{for } i \leq 1, \\ 4\Phi_0\dot{\varphi}_0^{-1}\gamma i E\left(\frac{\pi}{2}, \sqrt{1-i^{-1}}\right) & \text{for } i \geq 1. \end{cases}$$

If $i = 1$, the period $T = 2\pi/\omega_0$ and the equations of motion of the links have the form $\varphi = \Phi_0 \sin \omega_0 t$, $\psi = -\Phi_0 \cos \omega_0 t$, where $\omega_0 = \dot{\psi}_0/\Phi_0$ is the circular frequency.

Thus, two identical masses coupled by a transmission with transfer function (3) form a harmonic oscillator. Its properties differ from those of a potential-system harmonic oscillator. Thus, while the traditional harmonic oscillator has a natural frequency and an amplitude that depends on initial conditions, the amplitude Φ_0 is constant in the system considered here and the initial conditions, which determine the total kinetic energy, specify the frequency, i.e., the system is not isochronous. Figure 3a shows the transfer function and phase diagram for $i = 1$. Figure 3b reflects the influence of the inertia parameter on the phase paths for $I_2 = \text{const}$ and $E_0 = \text{const}$.

Let us consider the behavior of the oscillatory system in the presence of dissipative resistances reduced to the shaft of the first flywheel ($M_2 = 0$). In the cases of Coulomb, linear, and square-law friction, the moment of the resistance forces $M_1 = M$, $M_1 = \alpha_0 \varphi$, $M_1 = \beta_0 \varphi^2$, respectively, where M, α_0, β_0 are constants and Eq. (1) has a solution of the form $\varphi_{D_j}(n, \varphi) = \varphi_{\pm}(\varphi) D_{j\pm} \times (n, \varphi)$, where $j = 0, 1, 2$, respectively, for Coulomb, linear, and square-law resistance; $D_{j\pm}$ is the damping coefficient and n is the cycle number.

For Coulomb friction (Fig. 4a), we have $D_{0+}(n, \varphi) = \sqrt{1 - \mu [2(n-1)\Phi - \Phi_1 + \varphi]}$, $D_{0-}(n, \varphi) = \sqrt{1 - \mu [(2n-1)\Phi + \Phi_2 - \varphi]}$, where $\mu = 2M/I_2\dot{\psi}_0^2$.

Since D_0 decreases from 1 to 0 as n increases, the damping phase path is found to be inscribed into the path of the conservative system, is pulled toward the segment $[\Phi_1, \Phi_2]$ (the amplitude of the oscillations), passing across its ends, and terminates on it (Fig. 4a).

For linear friction (Fig. 4b), $D_{1+}(n, \varphi) = 1 - \alpha [(n-1)V + V_+(\varphi)]$, $D_{1-}(n, \varphi) = 1 - \alpha [(n-1)V + V_-(\Phi_2) + V_-(\varphi)]$, where

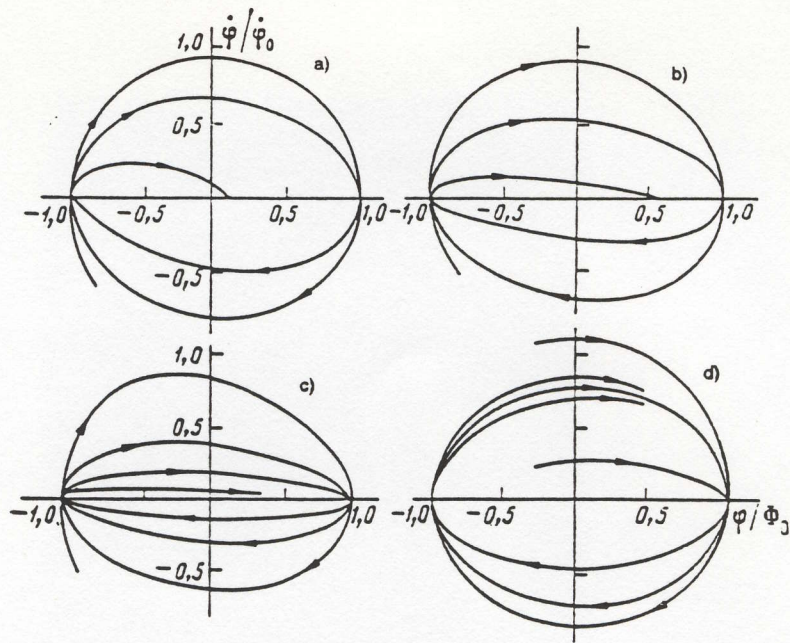


Fig. 4

$$V_+(\varphi) = \int_{\varphi_1}^{\varphi_2} (i_+ + u_+^2)^{-0.5} d\varphi, \quad V_-(\varphi) = \int_{\varphi_1}^{\varphi_2} (i_- + u_-^2)^{-0.5} d\varphi,$$

$$V = V_+(\Phi_2) + V_-(\Phi_1), \quad \alpha = \alpha_0 / I_2 \psi_0.$$

In this case, the damping coefficient depends on the form of the transfer function. Figure 4b shows the phase path for transfer function (3) and $i = 1$.

For square-law friction (Fig. 4c), $D_{2+}(n, \varphi) = \exp \{ \beta [(n-1)W + W_+(\varphi)] \}$, $D_{2-}(n, \varphi) = \exp \{ \beta [(n-1)W + W_+(\Phi_2) + W_-(\varphi)] \}$, where

$$W_+(\varphi) = \int_{\varphi_1}^{\varphi_2} (i_+ + u_+^2)^{-1} d\varphi, \quad W_-(\varphi) = \int_{\varphi_1}^{\varphi_2} (i_- + u_-^2)^{-1} d\varphi,$$

$$W = W_+(\Phi_2) + W_-(\Phi_1), \quad \beta = \beta_0 / I_2.$$

The phase path of this case for transfer function (3) is shown in Fig. 4c. In contrast to the previous cases, the nature of damping does not depend on the initial conditions, since the speed ψ_0 does not enter into $D_{2\pm}$. The segment $[\Phi_1, \Phi_2]$ which the phase path approaches asymptotically, passing across its ends, is analogous to the focus in potential system with linear friction.

The time of the n -th cycle in damping is determined from the formula

$$T_{D_n} = \int_{\varphi_1}^{\varphi_2} \frac{d\varphi}{\dot{\Phi}_{D_{2+}}(\varphi)} - \int_{\varphi_2}^{\varphi_1} \frac{d\varphi}{\dot{\Phi}_{D_{2-}}(\varphi)}$$

For small values of μ , α and β , the damping coefficients can be treated as varying little from cycle to cycle and can be taken out from under the integral sign. We then obtain approximate formulas for the time of the n -th cycle for $n \gg 1$: $T_{D_n}(n) \approx T / \sqrt{1 - 2\mu n \Phi}$, $T_{D_1}(n) \approx T / (1 - n\alpha V)$, $T_{D_2}(n) \approx T \exp \beta n W$.

The most important property of the inertia-type recuperative drive as an oscillatory system is the possibility of sustaining the oscillations with an external nonperiodic energy source, i.e., the possibility of setting up self-sustained oscillations. Thus, when a motor that can be reversed automatically at positions Φ_1 and Φ_2 and develops a constant torque M_e is introduced into a dissipative system with square-law resistance, the oscillations tend to a stable limit cycle $\psi_a = \psi_{a0} \omega_z$ (Fig. 4d), where

$$\psi_{a,0} = \sqrt{2M_e B / I_2 [\exp(2\beta W) - 1]}, \quad B = \int_{\Phi_1}^{\Phi_2} \{ \exp[2\beta W_+(\varphi)] + \exp(2\beta [W_+(\Phi_2) + W_-(\varphi)]) \} d\varphi.$$

We also note the possibility of setting up steady-state self-sustained oscillations with a nonreversible motor.

The oscillatory properties of the drive are clearly illustrated by a model in the form of a material point moving along the closed-path position function of the transfer mechanism and plotted in the scale μ_L in coordinates $x = \mu_L \bar{y} i \varphi$, $y = \mu_L \psi$. The equation of motion of this point $m v dv + X dx + Y dy = 0$ agrees with (1) if the mass of the point $m = I_1 / \mu_L^2 i$, and its velocity $v = \dot{x} \cos \kappa$, where κ is the angle between the vectors v and \dot{x} ($\tan \kappa = y_x'$) and the components of the external forces are $X = M_1 / \mu_L \bar{y} i$, $Y = M_2 / \mu_L$. The projections of the velocity v onto the axes correspond to the drive-mass velocities $\dot{x} = \mu_L \bar{y} i \dot{\varphi}$, $\dot{y} = \mu_L \dot{\psi}$. Rotational motion of the point in the model corresponds to oscillatory motion of the recuperator.

It is obvious that for the conservative system ($v = \text{const}$), the period of the oscillations can be interpreted as the perimeter of the closed path. For example, for the function (3), which represents a circle in x, y coordinates, the path for $i = 1$ is an ellipse whose perimeter is determined by formulas that correspond to (4). If $i = 1$, the point in the model moves along a circle. Obviously, the projections of its velocity onto the x and y axes vary harmonically. For a hinged four-link with a nearly elliptical position function, the period of the oscillations is given with high accuracy by the approximate formula for the perimeter of an ellipse with axes $2c = \mu_L \bar{y} i \Phi$, $2b = \mu_L [\psi(P_1) - \psi(P_2)]$: $T \approx \pi [1.5(c+b) - \sqrt{cb}]$.

This analysis of the recuperative drive points to the conclusion that an oscillatory system based on it (an inertia-type kinematic oscillator) will possess several properties useful for vibration machines. These properties include: the absence of an equilibrium position, a natural frequency, and variation of frequency with amplitude as a result of absence of elastic links, amplitude independent of initial conditions and mass of links, the possibility of setting up steady-state self-sustained oscillations in a broad frequency range, and the possibility of optimizing the motion of the final link by adjusting the transfer function.

Constant mechanism amplitude is important in the design of cyclic-action transport machines for automated systems: manipulators [7], turntables, dampers, etc. Thus, the power requirement of a working manipulator model with a lifting capacity of 0.63 kg based on an inertia-type recuperative drive is an order of magnitude lower than the power requirement of its analogs, and is much lighter and more compact. It would seem a promising idea to combine two or more final links into such a system and generate oscillations by exchanging kinetic energy between them. Vibration machines of this type would require no energy accumulators at all, and would eliminate the difficulties associated with resonance and the excitation and maintenance of vibrations at an arbitrary technologically optimal frequency and constant amplitude, as is often necessary [8]. It would be possible in mechanisms with many final links to set up wave motions with successive exchanges of kinetic energy between links.

REFERENCES

1. A. I. Korendyasev, B. L. Salamandra, and L. I. Tives, "Aspects of the design of kinematic schemes for automatic manipulators," *Stanki i Instrument*, no. 2, pp. 3-5, 1981.
2. T. S. Akinfiev, V. I. Babitskii, and V. L. Krupenin, "Resonant-type manipulator systems," *Mashinovedenie [Soviet Machine Science]*, no. 1, pp. 3-8, 1982.
3. I. I. Blekhman (Editor), *Vibrations in Engineering. A Handbook. Vol. 2. Vibrations of Nonlinear Mechanical Systems [in Russian]*, Mashinostroenie, Moscow, 1979.

4. I. I. Vul'fson and M. Z. Kolovskii, Nonlinear Problems in Machine Dynamics [in Russian], Mashinostroenie, Leningrad, 1968.
5. N. V. Gulia and I. D. Yudovskii, A Mechanical-Energy Recuperator. Soviet Patent No. 530132 [in Russian]. B. I., no. 36, 1976.
6. N. V. Gulia, A Discrete Variable-Ratio Belt Transmission Mechanism. Soviet Patent No. 171607 [in Russian]. B. I., no. 11, 1965.
7. I. D. Yudovskii, "A recuperative flywheel drive for nonreprogrammable automatic manipulators," Vestnik Mashinostroeniya, no. 4, pp. 9-11, 1985.
8. V. V. Gortinskii, "Technical level and prospects for development of vibration machines for the milling and food industries," Mashinovedenie [Soviet Machine Science], no. 1, pp. 3-7, 1985.

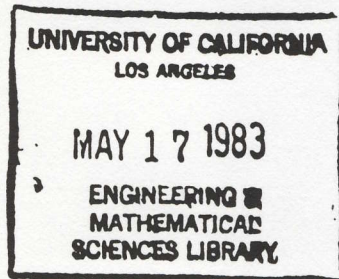
24 November 1988

Kiev

ISSN 0038-5298

Russian Original Vol. 18, No. 9, September, 1982

March, 1983

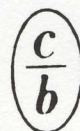


SOAMBT 18(9) 771-862 (1982)

SOVIET APPLIED MECHANICS

ПРИКЛАДНАЯ МЕХАНИКА
(PRIKLADNAYA MEKHANIKA)

TRANSLATED FROM RUSSIAN



CONSULTANTS BUREAU, NEW YORK

SOVIET APPLIED MECHANICS

A translation of *Prikladnaya Mekhanika*

March, 1983

September, 1982

Volume 18, Number 9

CONTENTS

	Engl./Russ.	
Energy Criteria of the Brittle Fracture of Materials with Initial Stresses — A. N. Guz'...	771	3
Scale Effect Regarding the Elastic Properties of Polycrystalline Materials — V. A. Lomakin, L. V. Kuksa, and Yu. N. Bakhtin.....	776	10
Wave Motions of Circular Cylindrical Shells — V. D. Kubenko, P. S. Koval'chuk, and N. P. Podchasov.....	781	16
Investigation of the Stress State of Inhomogeneous Cylindrical Shells — A. T. Vasilenko and N. D. Pankratova.....	787	23
Stress-Strain State of Reinforced Cylindrical Shells under Local Loading — D. E. Lipovskii and K. Z. Yagudin.....	793	30
Axisymmetric Thermoplastic State of Laminar Shells on the Basis of the Theory of Small-Curvature Processes — M. E. Babeshko, L. V. Prokhorenko, and A. Z. Galishin.....	797	35
Compatibility Conditions of Cylindrical Shells with a Low Shear Stiffness — I. G. Strel'chenko.....	802	41
Investigation of the Creep of Thin-Walled Shells under Nonstationary Loading — A. A. Zolocheskii and O. K. Morachkovskii.....	807	47
Investigation of the Stability of Compressed Cylindrical Shells with Thin Eccentric Ribs with a Polynomial Approximation of Deflections — A. S. Fainshtein.....	810	51
Solving Dynamic Problems of Viscoelasticity by Method of Amplitude-Differential Approximation — I. K. Senchenkov.....	815	57
Difference Equations in Strength and Stability Problems of Plates — R. F. Gabbasov	820	63
Stability of the Elastic Equilibrium of an Unbounded Plate in the Vicinity of an Arbitrarily Oriented Rectilinear Crack for a Plane-Stress State — G. G. Kuliev and É. N. Mamedov	824	68
Multilayer, Freely Supported, Trapezoidal Plates — I. Yu. Kolesnikov	828	73
Optimal Problem Connected with the Motion of a "Flywheel" Elevator — N. V. Gulia, M. Yu. Ochan, and I. D. Yudovskii.....	832	78
Dynamic Characteristics of Air Bearings — O. B. Milovanova, O. N. Chekin, and M. Sh. Dyshel'.....	837	84
Calculation of Defectiveness Buildup during Accelerated Fatigue Tests by Methods of Increasing Load — O. B. Balakovskii.....	841	90
Calculation of Ultimate State of Heat-Resistant Alloys under Long-Cycle Load — V. P. Golub and L. I. Ishchenko.....	846	95
Optimization of the Free-Vibration Damping Factor for a Linearly Distributed Two-Element System — A. V. Stepanov	851	102
Influence of Unbalance of a Dynamically Tuned Vibratory Gyroscope on Its Dynamics and Precision — A. V. Zbrutskii and M. A. Pavlovskii.....	855	107

The Russian press date (podpisano k pechati) of this issue was 9/14/1982.
Publication therefore did not occur prior to this date, but must be assumed

OPTIMAL PROBLEM CONNECTED WITH THE MOTION
OF A "FLYWHEEL" ELEVATOR

N. V. Gulia, M. Yu. Ochan,
and I. D. Yudovskii

UDC 621.01

In connection with the development of high-rise buildings, it has become a serious problem to ensure the evacuation of people during a fire from the upper stories of tall buildings that are beyond the reach of telescoping ladders from fire engines [3]. Among the equipment intended for the emergency evacuation of people, a promising mechanism is the "flywheel" elevator [1], which is shown schematically in Fig. 1. The load to be lowered 1 is attached to the end of a flat belt 2 that is wound onto a reel 3 attached to the shaft of a flywheel 4. As the load descends, the belt unwinds from the reel, decreasing its radius. The impact velocity depends on the radius of the reel at the end of the descent and the moment of inertia of the flywheel. By selecting these values we can ensure that the impact velocity can be made as small as any value specified in advance. After impact and the disconnection of the load from the belt, the device can be lifted rapidly and rewound on the shaft by using the energy that was stored in the flywheel during the descent. Then, the device is ready for the next descent.

Since one device is needed to ensure the consecutive descent of several people, it is important that the action be rapid. Because the descent time is considerably greater than the time necessary to lift the belt back up (the rise time), a problem to consider is how to ensure the most rapid descent of the load by means of the flywheel elevator. In order to vary the law of motion of the load over a sufficiently wide range, we can use a belt of variable thickness, which is obtained by gluing a covering to the underlying belt, as was done, for example, in [2].

The following problem arises. It is necessary to synthesize a mechanism that ensures the fastest descent of a load of mass m from a height H , such that the following conditions are satisfied: 1) the impact velocity of the load should not exceed v_0 ; 2) the acceleration during the damping should be no less than $-w_{per} \leq 0$; 3) the limiting permissible values of the shaft radius R are limited by certain given, positive quantities whose squares equal a and b ($a < b$); 4) the thickness of the belt should not be less than h_0 . The determination requires the moment of inertia of the flywheel I reduced to the shaft of the reel, the initial radius of the reel, and the profile of the belt.

From the law of conservation of energy, neglecting the mass of the belt and the dissipative losses, we determine the velocity of the load

$$v^2(l) = 2mg \int P(l) / [I + mP(l)], \quad (1)$$

where $P(l) = R^2(l)$; l is the coordinate of the load, and g is the acceleration of free fall.

For large heights, when the problem of optimization has some meaning, we have $I \gg mP(l)$. Then, to determine the velocity of the load we obtain

$$v^2(l) = 2mg \int P(l) / I. \quad (2)$$

We compare the values of the velocities from Eqs. (1) and (2). Their ratio $\epsilon = \sqrt{1 + mP(l)/I}$ is a maximum for $P(l) = b$ and for minimum I , which ensures attainment at the end of the descent of the velocity v_0

$$\epsilon_{max} = \sqrt{1 + bv_0^2 / (2gH - v_0^2)a}.$$

The quantities a and b are determined from structural considerations (a is limited by the flexural rigidity of the belt and b by the size of the mechanism), so that we usually have $a/b \leq 100$. The impact velocity is the same for descent from different heights ($v_0 = 1, 5, \dots, 2$ m/sec). As can be seen, as H increases, ϵ_{max} approaches unity. Thus, for actual structures, $\epsilon_{max} = 1.1$ for $H = 100$ m, and $\epsilon_{max} = 1.05$ for $H = 200$ m. Hence, for large H , Eq. (2) gives values for the velocity that differ little from the exact values of Eq. (1).

Institute of Engineering, Academy of Sciences of the USSR, Moscow. Translated from *Prikladnaya Mekhanika*, Vol. 18, No. 9, pp. 78-83, September, 1982. Original article submitted March 27, 1980.

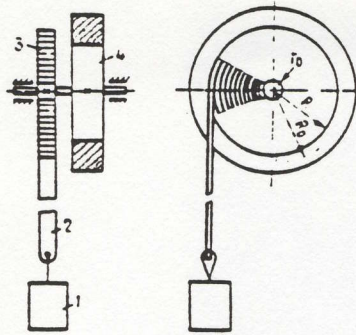


Fig. 1

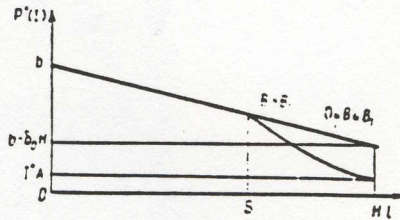


Fig. 2

The geometric relations for the rewinding of the belt are characterized by the function

$$P'_l(l) = -\delta(l) \quad (3)$$

or in integral form

$$P(l) = P(0) - \int_0^l \delta(l) dl, \quad (4)$$

where $\delta(l) = h(l)/\pi$; $h(l)$ is the thickness of the belt.

Differentiating (2) with respect to time and transforming, accounting for (3), for the acceleration of the load we obtain

$$w(l) = [P(l) - l\delta(l)]mg/l. \quad (5)$$

Conditions 1) and 2) taking into account Eqs. (2) and (5) assume the form $v_0^2 \geq 2mgHP(H)/I$; $-w_{per} \leq [P(l) - l\delta(l)]mg/l$. The time of descent is determined from the equation

$$t = \int_0^H \frac{dl}{v(l)} = \sqrt{\frac{I}{2mg}} \int_0^H \frac{dl}{\sqrt{IP(l)}}.$$

Taking into account the relations obtained, we have the following mathematical formulation of the problem. The functions $\delta(l)$ and $P(l)$ are connected by the relation (3), and superimposed on these functions are the constraints corresponding to conditions 1)-4)

$$P(H) \leq IA; \quad (6)$$

$$P(l) - l\delta(l) \geq -Bl; \quad (7)$$

$$0 < a \leq P(l) \leq b; \quad (8)$$

$$\delta(l) \geq \delta_0 > 0. \quad (9)$$

where $A = v_0^2/2mgH > 0$; $B = w_{per}/mg \geq 0$; and a , b , and δ_0 are certain given positive quantities.

Out of all the functions that are piecewise-continuous on the segment $[0, H]$ it is necessary to find functions $\delta(l)$ and $P(l)$, and also values of the parameter I that will ensure a minimum of the functional

$$\tau = \int_0^H \sqrt{I/IP(l)} dl. \quad (10)$$

We should note that the constraints (8) and (9) and Eq. (4) are compatible only when the following inequality is satisfied:

$$b - \delta_0 H > a. \quad (11)$$

We will call the functions $\delta(l)$ and $P(l)$ and the parameter I that minimizes the functional (10) optimal, and we denote them in terms of $\delta^*(l)$, $P^*(l)$, and I^* , and the value of the functional in terms of τ^* corresponding to them.

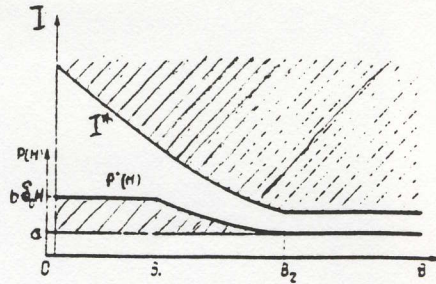


Fig. 3

We show that the optimal solution is the following. The parameter I^* is the minimum possible value out of all the values of I that do not contradict the constraints of the problem. For the functions $\delta^*(l)$ and $P^*(l)$, depending on the values that enter into the conditions, there are two cases possible.

1. For $B \geq B_1$, where B_1 is a certain quantity characterizing the initial data, the sought functions consist of two segments separated by a certain point with coordinate S . For $l \in [0, S]$ $\delta(l) = \delta_0$, $P^*(l) = b - \delta_0 l$, and for $l \in [S, H]$ the sought functions satisfy the algebraic equation

$$i\delta^*(l) - P^*(l) = I^*B \quad (12)$$

and differential equation (3) with boundary condition

$$P^*(H) = I^*A. \quad (13)$$

The value of S is determined from the condition of continuity of the function $P^*(l)$ at point S .

2. For $0 \leq B \leq B_1$, the sought functions consist of only the first segment, i. e., for them we have $S = H$. The form of the function $P^*(l)$ is shown in Fig. 2 for various B .

The indicated form of the optimal solution is found heuristically from the following physical considerations. The quickest descent corresponds to motion of the load with maximum velocity, which is attained with minimum possible moment of inertia of the flywheel and maximum value for the radius of the reel. The latter is attained if the initial radius of the reel has the maximum permitted value and is decreased in the slowest way possible from among the possible methods, i. e., by the winding of a belt of thickness δ_0 until the beginning of damping with minimum permissible acceleration $-w_{per}$ leading to impact with velocity v_0 . The second case ($0 \leq B \leq B_1$) holds for small w_{per} when the remaining quantities that enter into the conditions are fixed. It is characterized by the fact that for satisfaction of the constraint (7) the moment of inertia of the flywheel and the radius of the reel at the end of the descent will be so large that the impact velocity will be less than v_0 , and the section of variable thickness will be absent.

We assume that there exist certain other functions $\tilde{\delta}(l)$ and $\tilde{P}(l)$ satisfying constraints (6)-(9), and also the other parameter I , which give the value $\tilde{\tau} < \tau^*$ for the integral (10). Then

$$\tau^* - \tilde{\tau} = \int_0^H \left[\frac{1}{I^* P^*(l)} - \frac{1}{\tilde{I} \tilde{P}(l)} \right] \frac{dl}{l} > 0.$$

which leads to the inequality

$$\tilde{P}(l) - i P^*(l) > 0 \quad (i = \tilde{I}/I^*). \quad (14)$$

Note that according to the definition of I^* we have $i \geq 1$.

We show that it is impossible for inequality (14) to be satisfied at a single point of the segment $[0, H]$.

We consider the segment $[0, S]$. Substituting the value of $P(l)$ from (4) into (14) and separating i into the sum $i = 1 + \Delta$ ($\Delta \geq 0$), we obtain

$$\int_0^S [\delta_0 - \tilde{\delta}(l)] dl > (b - \delta_0) \Delta + b - \tilde{P}(0). \quad (15)$$

The first term on the right side of (15) is positive by virtue of (11), and the second — by virtue of constraint (8). Hence the integral on the left side of the inequality is positive, which contradicts the constraint (9).

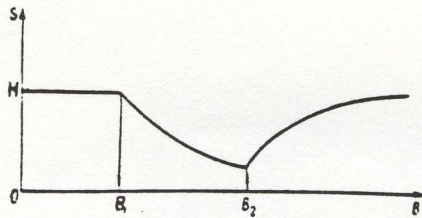


Fig. 4

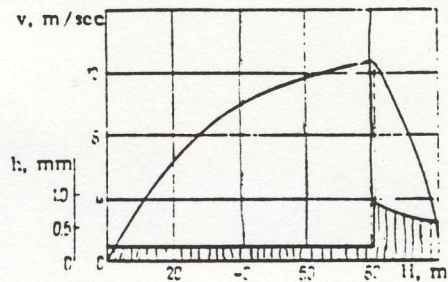


Fig. 5

Thus, on the segment $[0, S]$, inequality (14) is not satisfied. In particular, this is also true for $S = H$. So for $0 \leq B \leq B_1$, when the sought function consists of only the single section $o^*(l) \equiv o_0$, it is proved that it is impossible for a functional $\tilde{\tau} < \tau^*$ to exist. Because inequality (14) is not satisfied at any point of the segment $[0, S]$ it also follows that

$$\tilde{P}(S) - iP^*(S) \leq 0. \quad (16)$$

We now consider the segment $[S, H]$. We introduce the auxiliary function

$$y(l) = [\tilde{P}(l) - iP^*(l)]l, \quad (17)$$

which must be positive in order to satisfy (14). We let inequality (14) be satisfied at the point l_1 , i. e., $y(l_1) \geq 0$.

For satisfaction of the constraints $y(l)$ we cannot assume arbitrary values at the ends of the segment $[S, H]$. From (16) it follows that $y(S) \leq 0$. On the other hand, taking into account (11) and constraint (6), we have $y(H) = [\tilde{P}(H) - iP^*(H)] \leq (\tilde{I}A - iI^*A)H = 0$, i. e., $y(H) \leq 0$.

Thus, $y(l)$ is not positive at the ends of the segment $[S, H]$, and within the interior there exists a point at which $y(l_1) > 0$. By virtue of the continuity of the function $y(l)$ there exists a segment $[\alpha, \beta]$ including the point l_1 within which $y(l) > 0$ everywhere, with $y(\alpha) = y(\beta) = 0$. Differentiating (17), with accounting for (3) and (12), we obtain $y'(l) = \tilde{P}(l) - l\delta(l) + I^*Bl$. If we now use constraint (7) and the fact that $i \geq 1$, we arrive at the conclusion that $y'(l) \geq 0$. It is clear that

$$y(l) = y(\alpha) + \int_{\alpha}^l y'(l_x) dl_x.$$

Let $y'(l) \equiv 0$ for all $l \in [\alpha, \beta]$. Since $y(\alpha) = 0$, we conclude that $y(l) \equiv 0$ on the segment being considered, which contradicts the assumption that the function $y(l)$ is positive. We now assume that there exist certain values of l for which $y'(l) > 0$. Then for $l_2 = \beta$ the integral on the right side is strictly positive. At the same time, $y(\beta) = 0$ and, hence, the assumption made is not valid. Therefore, inequality (14) is not satisfied over the entire segment $[S, H]$.

Thus, it has been proved that there do not exist satisfactory constraints on the functions $\delta(l)$ and $P(l)$ and the parameter I , differing from those assumed, for which the integral (10) is less than τ^* . We now determine the values of the functions $\delta^*(l)$ and $P^*(l)$ and the parameter I^* .

From the parameter I^* we made use of only the information that it is the minimum of all the values of I satisfying the constraints. From inequality (7) for $l = H$ we have

$$BI \geq H\delta(H) - P(H). \quad (18)$$

We show that the values of I for which inequalities (6) and (18) are satisfied cannot be less than the quantity I^* given by the equations

$$I^* = a/A \quad (B \geq B_2); \quad (19)$$

$$I^* = \delta_0 H / (A + B) \quad (0 \leq B \leq B_2). \quad (20)$$

where B_2 corresponds to the equality of the values of I^* from (19) and (20)

$$B_2 = A(\delta_0 H/a - 1).$$

From constraint (6) with account of (8) for the assumed values of I^* we obtain

$$P^*(H) = a \quad (B \gg B_2); \quad (21)$$

$$a \leq P^*(H) \leq \delta_0 H A / (A + B) \quad (0 \leq B \leq B_2). \quad (22)$$

For $B \geq B_2$ we let there be a certain moment of inertia $\tilde{I} = i_1 a / A$ ($i_1 < 1$) and the value $\tilde{P}(H) = k_1 a$ that corresponds to it, where k_1 is an arbitrary coefficient. Substituting \tilde{I} and $\tilde{P}(H)$ into constraint (6), we obtain $k \leq i_1 < 1$, i. e., $\tilde{P}(H) < a$, which contradicts constraint (8). For $0 \leq B \leq B_2$, assuming that $\tilde{I} = i_1 \delta_0 H / (A + B)$ and $\tilde{P}(H) = k_2 \delta_0 H A / (A + B)$, from condition (6) we obtain $k_2 \leq i_1 < 1$. If we now substitute \tilde{I} and $\tilde{P}(H)$ into (18) and we convert, with account of inequalities (9) and (22), we have $i_1 B + k_2 A > A + B$, which is incompatible with the condition $k_2 \leq i_1 < 1$. Hence, it is not valid to assume that it is possible for \tilde{I} to be less than I^* . Thus it is shown that, independent of the form of the functions $\delta(l)$ and $P(l)$, the parameter I cannot be less than I^* , depending on the initial data and the constraints according to Eqs. (19) and (20).

We also establish an additional constraint on the quantity $P(H)$. Considering (4) for $l = H$ with account of constraints (8) and (9), we arrive at the inequality

$$P(H) \leq b - \delta_0 H. \quad (23)$$

With decreasing B the upper boundary of $P(H)$ from (22) increases and attains the limiting value from (23) for $B_1 = A(2\delta_0 H - b) / (b - \delta_0 H)$. Hence, for $0 \leq B \leq B_1$, it is necessary to allow for $P(H)$ the range of possible values $a \leq P(H) \leq b - \delta_0 H$. The boundaries obtained for I and $P(H)$ are given in Fig. 3.

We find the $\delta^*(l)$ law on the segment $[S, H]$ and the value of the coordinate S . Substituting $\delta^*(l)$ from (3) into (12), we obtain a differential equation in $P^*(l)$, the solution of which, taking account of the boundary condition (13), will be the function

$$P^*(l) = (A + B) I^* H / b - I^* B. \quad (24)$$

When this is differentiated, according to (3) we obtain

$$\delta^*(l) = (A + B) I^* H / l^2. \quad (25)$$

We find the value of the coordinate S from the condition of continuity of the function $P^*(l) - P_1^*(S) = P_2^*(S)$, where $P_1(S)$ and $P_2(S)$ are the values of the function on the sections $[0, S]$ and $[S, H]$, which have already been found. Hence, we have the equation $b - \delta_0 S - (A + B) H I^* / S + I^* B = 0$, whose roots are

$$S_{1,2} = 0.5 [b + B I^* \pm \sqrt{(b + B I^*)^2 - 4 \delta_0 (A + B) I^* H}] / \delta_0.$$

We assume that the point of switching is given by the coordinate $S_1 > S_2$. We consider the function $y_1(l) = l [P_1^*(l) - P_2^*(l)]$, which, on the segment $[S_1, S_2]$ with account of (4) and (24), equals $y_1(l) = -\delta_0 l^2 + (b + B I^*) l - (A + B) I^* H$. Since S_1 and S_2 are its roots, in the interval (S_1, S_2) , the quantity $y_1(l) > 0$, i. e., $y_2(l)$ is a particular case of the function (17) for $\tilde{P}(l) = P_1^*(l)$, $i = 1$, $\alpha = S_1$, $\beta = S_2$ and, hence, its existence is also impossible, and the sought value of S is

$$S = 0.5 [b + B I^* - \sqrt{(b + B I^*)^2 - 4 \delta_0 (A + B) I^* H}] / \delta_0.$$

The value of the coordinate S as a function of B is represented in Fig. 4.

By substituting the optimal values obtained for the functions $\delta^*(l)$ and $P^*(l)$ and the parameter I^* into expressions (6)...(9), we can verify that they agree with the conditions of the problem.

As an example we synthesize the mechanism that executes the quickest descent of the load for $m = 100$ kg, $H = 100$ m, $v_0 = 2$ m/sec, $w_{per} = 4$ m/sec², $h_0 = 0.2$ mm, $a = (10 \text{ mm})^2 = 10^{-4}$ m², $b = (100 \text{ mm})^2 = 10^{-2}$ m. For it we have $I = 5$ kgm², $R(H) = 0.01$ m, $S = 81$ m, $h(S) = 0.96$ mm, $h(H) = 0.63$ mm. The profile of the belt and the curve of the motion of the load are shown in Fig. 5.

LITERATURE CITED

1. N. V. Gulia, M. Yu. Ochan, I. D. Yudovskii, et al., Inventor's Certificate No. 827082 (USSR), Device for Descent. Bulletin of Inventors, No. 17 (1981).

1. N. V. Gulia and L. D. Yudovskii, "Synthesis of a belt for a discrete belt variant," *Izv. Vuzov., Mashinostroenie*, No. 7, 35-40 (1974).
2. A. S. Kataeva, *Rescue Equipment [in Russian]*, VNIPO MVD SSSR, Moscow (1976).

DYNAMIC CHARACTERISTICS OF AIR BEARINGS

O. B. Milovanova, O. N. Chekin,
and M. Sh. Dyshel'

UDC 539.3

It has been proposed [1] that air bearings be used for vibration testing of large and heavy beam and shell structures. The purpose of such a bearing is to take up the weight of the tested object, to provide the support platform of the object with necessary degrees of freedom, and to provide vibration isolation between the object and the ambient medium. Inasmuch as the air bearing is a component part of the "test object - air bearing" system, it adds its mass, stiffness, and energy dissipation to this system. These characteristics of an air bearing must be determined before their influence on the vibration characteristics of the test object can be evaluated. In an earlier study [2] data have been reported on various designs of air bearings, behavior of such bearings under static load, and dependence of their stiffness and dissipative properties on geometrical and physical parameters. In this study will be present data on the characteristics of air bearings under dynamic load.*

1. Tests were performed on singly connected and doubly connected air bearings with the same geometrical characteristics as before [2]. The tests were performed in a stand facilitating excitation of transverse vibrations of air bearings along the OX axis, longitudinal vibrations along the OZ axis, and torsional vibrations about both OX and OZ axes. The test of air bearings for longitudinal vibrations is shown schematically in Fig. 1. Two air bearings 14, separated by a spacer-plate 13, were placed between cross-arms 12 of the test stand. The pressure of compressed air entering the bearing cavity was recorded by manometer 11 and the axial force developed by the air bearings was measured with dynamometer 6. For exciting vibrations in the air bearings, the spacer-plate 13 has been rigidly connected in the middle to a special vibrator 8 consisting of two beams of rectangular cross section spaced symmetrically about its longitudinal axis and joined through three cross-arms: one at the center and one at each end. This construction of the vibrator makes it possible to vary its flexural stiffness by rotating the beams about their longitudinal axis and thus vary the frequency of vibrations. The vibrator was excited by an electromagnet 1 fed through a model LIT-2 inverter 2, the frequency of its vibrations being regulated by means of a model ZG-16 audio oscillator 3. The vibration process was recorded through BIL-type vibrators 4 on a model N-105 loop oscillograph 5. After the vibrations of the "air bearing-spacer-plate-vibrator" system have been tuned to resonance (as indicated by the signal on the oscillograph reaching its maximum), the plate supply of the inverter was switched off with the vibrations of the system changing, as a result, from steady ones to decaying ones. By changing the orientation of vibrator 8 and the point of its attachment relative to the spacer-plate 13, also by changing the direction of action of the exciting force, it was possible to realize all the four given modes of vibration in the air bearings.

The technical characteristics of the vibrator were: frequency range of natural flexural vibrations in the fundamental mode 8-18 Hz, logarithmic decrement of vibration amplitude 0.017, mass 265 kg. The

* This study, just as the earlier one, was performed under the guidance of S. V. Malashenko.

TABLE 1

Mode of mounting	1	2	3	4	5	6
f, Hz	18.8	18.7	18.4	18.0	18.4	18.7
δ	0.007	0.008	0.009	0.025	0.010	0.025

Institute of Mechanics, Academy of Sciences of the Ukrainian SSR, Kiev. Translated from *Priladnaya Mekhanika*, Vol. 18, No. 9, pp. 84-89, September, 1982. Original article submitted March 17, 1981.

mechanical sciences

MASHINOVEDENIYE

ISSN 0025-6536

2

1980

UNIVERSITY OF CALIFORNIA
LOS ANGELES

OCT 12 1981

ENGINEERING &
MATHEMATICAL
SCIENCES LIBRARY

*scientific information
consultants limited
london england*

MECHANICAL SCIENCES - MASHINOVEDENIYE

formerly MACHINE SCIENCE ABSTRACTS

English digest of the Soviet bimonthly MASHINOVEDENIYE

Published by Scientific Information Consultants Ltd.,
661 Finchley Road, London NW2 2HN, England.

Editors: Eugene Gros, Dipl. Ing., London.

Trevor Nettleton, M.Sc., C.Eng., M.I. Mech.E.,
Senior Lecturer, Mechanical Engineering Department,
City University, London.

2 / 1980

	Page No.	
	Original Russian article	Abridged English translation
Azbel' G. G., Rubin B. B. DYNAMICS OF VIBRO-IMPACT PILE DRIVING	3	3
Budanov B. V. ALLOWANCE FOR THE STIFFNESS OF THE FRICTION CONTACT IN VIBRATORY DISPLACEMENT THEORY	8	8
Kryukov B. I., Prosvirnin V. M., Seredovich G. I. ASYMMETRICAL HARMONIC OSCILLATIONS IN SYSTEMS WITH SYMMETRICAL NONLINEAR CHARACTERISTICS	13	14
Makarov B. P., Perov V. A., Troshenkov M. K. INVESTIGATION OF OPTIMAL NONLINEAR VIBRATION ISOLATION SYSTEMS UNDER RANDOM EXCITATIONS	16	18
Poznyak E. L. DAMPING OF FORCED OSCILLATIONS OF ROTORS ON PLAIN BEARINGS	21	24
Kavolelis A. - P. K. DYNAMICS OF FLEXIBLE CENTRIFUGAL COUPLINGS	26	30
Sverdlov S. Z. INVESTIGATION OF THE POSITIONING ACCURACY OF A PNEUMATIC DRIVE WITH DISCRETE CONTROL	33	38
Yudovskiy I. D. OPTIMUM BALLASTING OF WOUND FLYWHEELS	36	41
Karpovich S. E. OPTIMISING SYNTHESIS OF A SPATIAL GUIDING MECHANISM	40	46
Chaplygin M. V. ANALYTICAL APPROXIMATION OF EXPERIMENTAL CURVES	44	50
Bazhenov V. G., Kravchenko A. A., Ugodchikov A. G., Urzhuntsev I. P. ANALYSIS OF HARDENING STRESSES AND INVESTIGATION OF THEIR EFFECT ON THE BENDING STRENGTH OF GEAR WHEELS	46	53
Kutepova T. V. STRESS ANALYSIS OF THREADED JOINTS BETWEEN CYLINDRICAL SHELLS	53	60

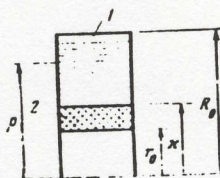
UDC 621.839
OPTIMUM BALLASTING OF WOUND FLYWHEELS

Yudovskiy I. D. (Moscow)

A criterion for the optimum value of ballasting of a wound anisotropic flywheel is considered, based on the condition of achieving the highest volume density of energy. Anisotropy coefficients are given for the cases most often encountered in practice. 4 figs., 3 refs.

Flywheels made by winding of high-strength filament and fibre materials are distinguished by high-energy density and safety against bursting. One of the problems arising in the development of these flywheels is maintaining the compactness of the wound rim under the action of centrifugal forces. A loss of compactness of the winding causes delamination and failure of the flywheel.

Fig. 1. Diagram of a wound flywheel with ballast:
1 - wound layer, 2 - ballast.



The most convenient method of preventing delamination is the loading of the inside surfaces of the flywheel with ballast which compresses the rim from the inside during rotation. An annular element 2 (Fig. 1) devoid of tangential stiffness, placed inside the wound rim 1, is often used as a ballast, for example, a set of segments or a heavy powder. In a flywheel, practical considerations usually determine the external diameter; in fact, they limit the volume of the element which concentrates the energy. The problem arises of selecting the inside radius of the flywheel and the relationships between the density of the ballast, its thickness, the density and thickness of the wound layer such that the maximum quantity of kinetic energy is accumulated in the effective volume of the flywheel, without exceeding the allowable stress, i. e. the problem is that of maximising the volumetric energy density of a ballasted flywheel subject to stress limitations. In this formulation of the problem the effective volume is understood as the total volume of a cylinder of given length bounded by the outside radius. If the flywheel is a hollow cylinder, then its effective volume contains the volume of the hollow space.

A cylindrical flywheel of unit thickness with the outside radius R_0 , inside radius r_0 , and inside radius of the wound layer κ is considered. The specific gravities of the winding and ballast materials are γ_H and γ_b respectively. The geometric dimensions of the flywheel are defined by the relative quantities $r = r_0/R_0$ and $x = \kappa/R_0$.

A coefficient of ballasting efficiency is introduced

$$K_b = e_w / T_{\max}, \quad (1)$$

where e_w is the energy density and T_{\max} are the maximum stresses.

For a rim of cylindrical shape

$$e_w = \frac{E}{w} = \frac{\gamma_e (R_0^4 - x^4) + \gamma_n (x - r_0^4)}{4R_0^4} \omega^2, \quad (2)$$

where E is the energy accumulated in the flywheel; $w = \pi R_0^2$ is its effective volume and ω is its angular velocity.

In Ref. 1, the radial stresses N and tangential stresses T were obtained for anisotropic wound rotor

$$N(\rho) = \gamma_e \omega^2 x^3 (-\alpha \rho^3 + C_1 \rho^{k-1} + C_2 \rho^{-k-1}), \quad (3)$$

$$T(\rho) = \gamma_e \omega^2 x^3 [-\beta \rho^3 + k(C_1 \rho^{k-1} - C_2 \rho^{-k-1})], \quad (4)$$

where $\alpha = (\nu_0 + 3)/(9 - k^2)$; $\beta = 3\alpha - 1$; $\rho = \rho_0/x$; ρ_0 is the variable radius (between r_0 and R_0); $k = \sqrt{E_t/E_r}$ is the anisotropy coefficient; E_t, E_r ; ν_0 are the elastic moduli in the tangential and normal directions and the Poisson ratio in the tangential direction.

The integration constants C_1 and C_2 can be obtained from the conditions that the stresses at the periphery vanish and that no delamination takes place, i. e. that no radial tensile stresses occur in the rim even at the smallest load on the windings caused by the bursting pressure of the ballast. These constants are found to be (Ref. 1)

$$C_1 = \frac{\alpha(k+3)}{2k} x^{k-1}, \quad C_2 = \frac{\alpha(k-3)}{2k} x^{-k-1}. \quad (5)$$

It is an essential fact that C_1 and C_2 depend on x . It should be noted that, if some radial tensile stresses are allowed in the wound material because of the presence of a bonding substance, the integration constants will acquire different magnitudes.

Assuming $\rho = 1$, Equation (3) yields the magnitude of the radial stress at the inside surface of the rim such that delamination is avoided, namely

$$N(1) = \gamma_e \omega^2 x^3 (-\alpha + C_1 + C_2). \quad (6)$$

This stress is created by the pressure N_0 of the ballast layer during the rotation of the rim.

Over a unit length of the periphery at the radius x , a force produced by a ring of the radius ρ_0 and the thickness $d\rho_0$ acts, namely $dN_0 = \gamma_e \omega^2 \rho_0 d\rho_0 / x$ hence, after integration, it follows that

$$N_0 = \frac{\gamma_e \omega^2}{3x} (x^3 - r_0^3). \quad (7)$$

Since $N_0 = -N(1)$, it follows from Equations (6) and (7) that the condition of the absence of delamination in the rim is

$$\gamma = \frac{3(\alpha - C_1 - C_2)}{1 - (r/x)^3} \quad (8)$$

where $\gamma = \gamma_b / \gamma_H$ is the relative density of the ballast material.

It follows from Ref. 1 that the largest tangential stresses in a ballasted flywheel arise at the inside surface of the rim (at $\rho = 1$) and these stresses, by virtue of Equation (4), are equal to

$$T_{\max} = \gamma \cdot \omega^2 x^2 [-\beta + k(C_1 - C_2)]. \quad (9)$$

Using Equations (1), (2), (9), the magnitude of the ballasting efficiency becomes

$$K_b = 0.25 \frac{1 - x^4 + \gamma(x^4 - r^4)}{x^4 |-\beta + k(C_1 - C_2)|}. \quad (10)$$

In the general case, an analytical examination of Equation (9) for the maximum value of T_{\max} as a function of the two variables r and x leads to a system of algebraic equations of high powers. However, for any concrete case of ballasting, it is always possible to calculate K_b numerically for different values of r , choose the optimum value and find the corresponding values of x and of the relative density γ .

By way of example, the condition of optimum ballasting of a flywheel wound of steel wire without bonding material will be determined. The dimension of the inside bore of the flywheel is not given. As will be shown below, the anisotropy coefficient for the case under consideration is $k = 2.0$.

Fig. 2 shows a family of $K_b(x)$ curves for $r = 0; 0.4; 0.6; 0.8$; obtained from Equations (5), (8), (10). It is seen that a maximum value of ballasting efficiency ($K_b = 0.278$) is achieved with $r = 0.6$, $x = 0.73$ and $\gamma = 2.23$. For steel wire, the maximum allowable stress is $T_{\max} = 3 \cdot 10^9$ N/m². With this stress, a unit of volume bounded by the bulk of the flywheel embodies an energy density $e_w = K_b T_{\max} = 0.834 \cdot 10^9$ J/m³. Assuming that the space factor of a wire wound rim is equal to 0.79, it follows that $\gamma_H = 0.79 \cdot 7.8 = 6.1$ g/cm³ and $\gamma_b = 2.23 \cdot 6.1 = 13.6$ g/cm³, the ballast can be made of uranium powder placed in a lead matrix (Ref. 3).

The anisotropy coefficient k will now be determined with greater accuracy for the most frequently used wound flywheels.

In winding flywheels from a strip or from rectangular section wire without intermediate layers of bonding material, this coefficient is equal to unity, because the elastic properties of the material in such a flywheel are equal in the radial and tangential directions. It is easily shown that, in the case of the presence of an embedding bonding substance, the anisotropy coefficient is

$$k = \sqrt{\left(\delta_s + \frac{E_c}{E_s} \delta_c\right) \left(\delta_s + \frac{E_s}{E_c} \delta_c\right)} / (\delta_s + \delta_c)^2,$$

where δ_s , δ_c are the thicknesses of the strip and of the bonding layer; E_s , E_c are their elastic moduli.

The magnitude of the anisotropy coefficient k will now be determined for the case when the rim is made of round section wire. Such a rim is wound on a spool with axial lay-up of the wire and constitutes wound cylinders nested in each other, where adjacent cylinders are wound in opposite senses.

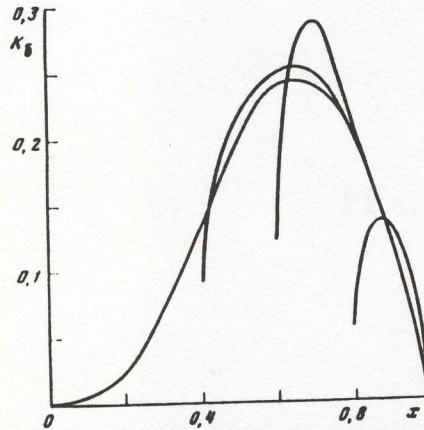


Fig. 2. Curves of the ballasting efficiency with different dimensions of the inside bore of the flywheel ($r = 0$; 0.4; 0.6; 0.8).

In the absence of a load which compresses the wire turns in a radial direction, these cylinders have a point contact. Under load, the contact spot acquires the shape of an ellipse, greatly extended along the wire axis. If the diameter of the rim is much larger than the diameter of the wire and of the winding pitch, the ellipse can be regarded as being extended so far that the contact spot degenerates into a contact band, i. e. the turns lie exactly above each other (Fig. 3). The intervals between the turns are filled with the bonding material which merely plays the part of fixing the positions of the winding turns. In studying the contact between turns in two adjacent layers of the winding, each turn is regarded not as a torus but as a cylinder, i. e. the radius of the turn is regarded as infinite. Thus, the problem is reduced to finding the displacement by compression between two parallel cylinders, making contact along their generating lines.

Fig. 3. Analytical model to determine the anisotropy coefficient for a wire or round section.



It is assumed that an element of the material is compressed across the winding by a force N , causing relative strains in the material in this direction, which are equal to ϵ . The elastic modulus in the radial direction when compressive stresses are present in the rim is obviously equal to $E_r = N/\epsilon$. The total deformation in the radial direction is the consequence of the approach between adjacent wires due to contact strains. The solution of the Hertz problem for the contact between two cylinders along their generating lines is (Ref. 2)

$$\delta = 0,579 \frac{q}{E} \left(\ln \frac{Ea}{q} + 2,06 \right), \quad (11)$$

where a is the wire radius; E is the modulus of elasticity of the wire material; q is the load per unit length of the wire.

If, in the element under examination, n cylinders are contained, then the total deformation of the element is $\delta(n-1)$, and the relative deformation is $\epsilon = \delta(n-1)/2an$. With large values of n , it can be assumed that $\epsilon = \delta/2a$. The load per unit of wire length is associated with the stress by the equation $q = 2aN$. Thus, $E_r = q/\delta$, and, taking account of Equation (11), it becomes $E_r = E/0,579 [1,357 + \ln(E/N)]$.

Assuming $E_0 = 0,79E$, the anisotropy coefficient k becomes

$$k = 0,676 \sqrt{1,357 + \ln(E/N)}. \quad (12)$$

The range of variation of k for real flywheel structures will now be considered. To this end, Equation (12) is rewritten in the form

$$k = 0,676 \sqrt{1,357 - \ln \eta \epsilon_{\max}},$$

where $\eta = N/T_{\max}$ is the ratio of the radial stress in the flywheel to the maximum tangential stress; $\epsilon_{\max} = E/T_{\max}$ is the relative strain of the rim in the tangential direction, equal to the maximum allowable strain of the wire.

For materials used in the manufacture of flywheels, $\epsilon_{\max} = 0,01 - 0,03$. Such a range of ϵ_{\max} variation practically does not reflect upon the magnitude of k .

The value of η varies from zero at the flywheel periphery to a certain maximum value at the inside surface of the rim, namely, $\eta_{\max} = |N_{\max}/T_{\max}|$. Equations (3) - (5) yield the following expression for η_{\max} :

$$\eta_{\max} = \left| \frac{1 - (k+3)x^{k+3}/2k - (k-3)x^{-k-3}/2k}{3 - (k+3)x^{k+3}/2 + (k-3)x^{-k-3}/2 - (9-k^2)/(v_0+3)} \right|. \quad (13)$$

In practice, the ratio of the inside radius of the winding to its outside radius varies within the limits or $x = 0,6 - 1,0$. With such a variation, it is seen from Equation (13) that, for k varying in the range between 1,5 and 2,5, η_{\max} does not exceed 0,1, i. e. the normal stresses in flywheels do not exceed 10% of the maximum tangential stresses. It is seen from the curve in Fig. 4 that the anisotropy coefficient of a wire wound flywheel differs little from the value $k = 2,0$, which should be adopted for stress analysis. The sharp rise of k at $\eta < 0,01$ is not taken into account because it occurs only in a few final windings.

Received: 24. IV. 1979.

BIBLIOGRAPHY

1. Guliya N. V., Ochan M. Yu. Theory of wound rotors. In book: Mechanics of Machinery. Issue 53. Moscow, "Nauka", 1978.
2. Rabenhorst D. W. The Multirim Super-Flywheel. Technical Memorandum. J. Hopkins University, August 1974, TG 1240.

Soviet Engineering Research

1986 Volume 5 Number 4

April

PERA

CALIFORNIA
FILES

FEB 22 1986

LIBRARY



Handwritten signature and date:
3/22/86

CONTENTS

	SER page	Vestnik page
DESIGN, TESTING AND RELIABILITY OF MACHINES		
Recuperative flywheel drive for non-reprogrammable automatic manipulators	<i>I. D. Iudovskii</i>	2 9
Vibration of overhead travelling-crane cabs	<i>A. L. Fedorov et al</i>	4 12
MECHANICAL ENGINEERING TECHNOLOGY		
Active tool wear check by acoustic emission method	<i>V. N. Poduraev et al</i>	6 14
Calculation of the required number of tools (replacements) for multi-tool machining under unmanned operation	<i>A. L. Vil'son, G. V. Samkharadze</i>	11 19
Flexible Automated Systems		
Flexible manufacturing systems: standard design solutions and future developments	<i>B. S. Belov et al</i>	15 24
General approaches to the analysis and synthesis of flexible automated manufacturing systems	<i>P. I. Chinaev</i>	18 27
Improving the reliability of flexible manufacturing systems	<i>S. V. Vasil'ev</i>	21 31
Automated grouping of components for flexible automated production	<i>V. M. Kushkov et al</i>	23 35
Computer controlled NC electrical discharge machine sections	<i>A. T. Kravets, A. F. Bogachev</i>	25 39
Software for the operative control of a flexible manufacturing system	<i>V. L. Erukhimovich et al</i>	26 40
A distributed control structure for FMS using a local computer network	<i>M. A. Mikhailovskii, M. Ya. Mogilevskii</i>	27 42
A programmable control switch with a control unit for drives in FMS equipment	<i>E. L. Tikhomirov et al</i>	28 44
Data processing in flexible automated production	<i>B. K. Tsukerman</i>	31 47
Effect of multi-machine tending on the efficiency of NC machine utilization in an FMS for small-batch and one-off production	<i>M. Kh. Blekherman, M. D. Margolin</i>	32 48
Transport — storage system based on combined linear electric motors	<i>M. M. Nikitin, V. A. Niyazov</i>	35 51
Investigation of the limiting characteristics of electrostatic gripping devices in robot technology	<i>V. N. Abrarov et al</i>	37 59
	SER Page	Stanki Page
PRODUCTION AUTOMATION		
The use of image recognition systems for automatic workpiece gauging	<i>V. G. Ostapchuk et al</i>	40 5
Selecting a rational equipment layout in a flexible manufacturing system	<i>S. S. Stoyanchenko</i>	42 7
A simulation model for assessing the positioning time of a robot	<i>D. R. Kriskii, V. Ya. Naimanov</i>	45 9
METAL-CUTTING MACHINE TOOLS		
Assessing the productivity of metal-cutting equipment	<i>V. S. Vasil'ev</i>	50 14
Screwcutting on multi-spindle automatic Lathes	<i>I. Ya. Mirnov, V. P. Kuznetsov</i>	54 16
Frequency division of errors of the kinematic chain of gear — cutting machines	<i>V. F. Ionak</i>	57 18
Increase of vibro-stability in turning machines	<i>G. N. Meshcheryakov et al</i>	58 19
Protective systems for preventing excessive cutting speeds during machining on longitudinal grinding machines	<i>Yu. N. Petrenko et al</i>	59 20
Sectioned type aerostatic spindle bearings	<i>Yu. A. Pikalov et al</i>	62 22
MACHINING		
Automation of cutting condition programming in CNC operative systems on cylindrical grinding machines	<i>V. I. Tartakovskii et al</i>	65 27
Control of linear and angular resilience deformations of flexible blanks during turning	<i>A. I. Bokhonstskii et al</i>	66 28

where $l = J_1/J_2$; $\alpha = k/J_2$.

To deal briefly with the case when the aerodynamic losses can be disregarded, from formula (2) velocity, acceleration and time of turn of the member 1 depend on the angle φ_1 in conformance with the formulae

$$\dot{\varphi}_1 = \omega(\varphi_1); \ddot{\varphi}_1 = \epsilon(\varphi_1); t = \tau(\varphi_1)/\dot{\varphi}_0,$$

where the functions $\omega(\varphi_1)$, $\epsilon(\varphi_1)$ and $\tau(\varphi_1)$ are analogs of the velocity, acceleration and time of turn which are linked to the angle φ_1 by the relationships

$$\omega(\varphi_1) = \frac{l}{\sqrt{l+u^2}}; \epsilon(\varphi_1) = \frac{-u u' \varphi_1}{l+u^2}; \tau(\varphi_1) = \int_0^{\varphi_1} \sqrt{l+u^2} d\varphi_1.$$

In Fig. 2 are shown the graphs of the analogs of the velocity ω and of the acceleration ϵ , and also a graph of the angle of turn φ_1 of the member 1, as a function of the analog of time τ for the mechanism with which the ratio l of the link rod length to the length of the arm equals 3, and $i = 1$. With a maximum angular velocity of $\dot{\varphi}_0 = 5s^{-1}$, and a corresponding angular velocity of the manipulators, the maximum acceleration $\ddot{\varphi} = 16,7s^{-2}$ and the time of turn is $t = 1,3s$. The angle of turn amounts in this case to $\psi = 233,13^\circ$.

In Fig. 3 are shown the dependences of ψ , τ and ϵ on the geometry of the four-link mechanism as expressed by the magnitude of l . It is important that when $l < 2,4$, the maximum acceleration of the member 1 is reached not at the boundaries of the cycle (curve ϵ_0) as it was the case in Fig. 2, but in the middle (curve ϵM). This makes it possible to synthesize drives, with which the braking force and acceleration reduces smoothly to the boundaries of the cycle, which is particularly useful for a reduction of the vibrations of the arm of the manipulator for a sharp

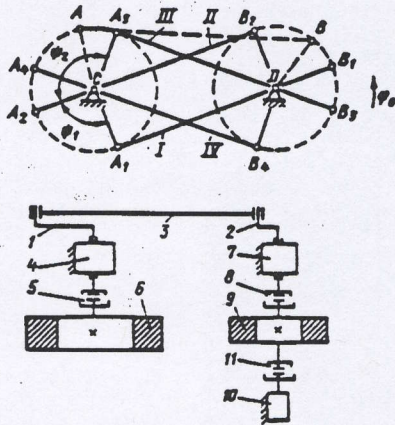


Fig. 1. Schematic diagram of a flywheel-lever recuperator.

change of the dynamic loads at the beginning and end of the motion.

The total angle of turn $\psi = 360^\circ - 2 \arctan(l-1)$ does not depend on the dynamics of the manipulator and is determined only by the lengths of the members of the four-link mechanism. Co-ordination of the angle of turn of the member 1 (Fig. 1) with the required angle of turn of the manipulator is ensured by a reduction gear 4.

The dynamic characteristics of the mechanism were checked experimentally on models of a device which performed recuperative braking both of revolving and of reciprocating masses.

The data quoted proves the possibility of an effective use of a flywheel-lever recuperator in drives of manipulators.

REFERENCES

1. BELYANIN, P. N. *Industrial robots*. Mashinostroenie, M., 1975, 136 pp.
2. AKINFIEV, T. S. et al. *Manipulator systems of the resonance type*. Mashinovedenie, No. 1, 1982, pp. 3-8.
3. KORENDYASEV, A. I. et al. *Features of the construction of kinematic circuits of automatic manipulators*. Machines and Tooling, No. 2, 1981, pp. 3-5.
4. AKINFIEV, T. S. *Resonance manipulator systems with electric drive*. Mashinovedenie, No. 6, 1983, pp. 18-23.
5. ARTOBOLEVSKII, I. I. *Theory of mechanisms*. Nauka, M., 1967, p. 195.

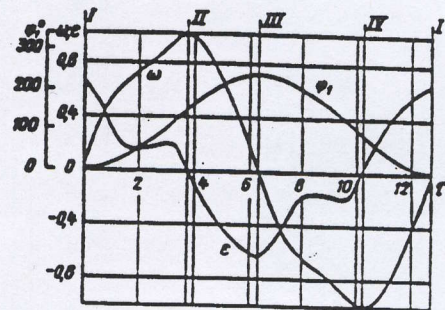


Fig. 2. Dependences of the angle of turn φ_1 , and the analogs of velocity ω and of acceleration ϵ on the analog of the time τ (I, II, III and IV are the characteristic positions of the members of a four-link mechanism).

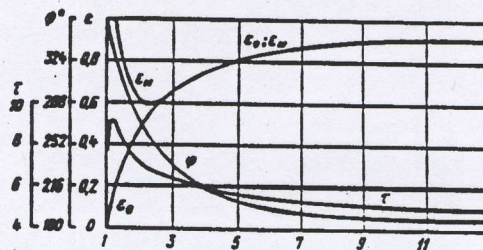


Fig. 3. Dependences of the total angle of turn ψ , of the analogs of acceleration at the start of the motion ϵ_0 and of the maximum acceleration ϵM and of the analog of the time τ on the dimensionless value of $l = AB/AC$.

The increase in the speed of action and the load carrying capacity of manipulators usually entails an increase of the power of the drives and of the damping devices, and also an increase in the energy consumption. The reduction of the cycle time for existing manipulators is limited by the demand for precision in the positioning of the moving members¹. When use is made of special positioning systems, the drive becomes complicated and its functional reliability is lowered. Moreover, when braking, the kinetic energy is converted to heat which often leads to the need for using devices for cooling and regulating heat to maintain the stability of the drive characteristics. At the same time, in a number of articles, for example by Akinfier and Korendyasev^{2,3}, it is suggested that a recuperative braking system for the moving components by used in manipulators. This provides a reduction in the power of the drive and the energy consumed, due to the use of the braking energy, which is stored in spring accumulators, for the next acceleration. The possibility of speeding up the drive action of a manipulator by an order of magnitude is mentioned by Akinfier⁴, which at the same retains its power thanks to the use of a recuperation system.

In addition to the recuperative drives for manipulators, use can be made of a flywheel-lever recuperator* for non-reprogrammable automatic manipulators and other mechanisms with a determinate displacement of the actuating element.

The recuperative flywheel drive which is shown in the diagram of Fig. 1 consists of the arms 1 and 2 and the link rod 3. The arm 1 is connected through the transmission 4 and the clutch 5 to members which effect one of the stages of mobility of the manipulator, e.g. rotation. On Fig. 1 these members are represented by the flywheel 6. The arm 2 is connected by the transmission 7 and the clutch 8 to the flywheel 9 which is an energy accumulator. The dissipative losses of energy are compensated by a motor 10.

The lengths of the members of the four-link mechanism are chosen such that when the arms are revolved from the extreme positions I, II, III, IV, the transmission ratio between them varies monotonically from 0 to $\pm \infty$. In particular, this occurs when the lengths of the arms 1 and 2 are the same and the length of the link rod 3 is such that when one arm is perpendicular to the link rod, the second lies on the same straight line as the link rod.

Turning now to an examination of such a drive, the clutches 5 and 8 are disengaged in the position of standstill of the manipulator members (the flywheel 6 is not moving), and the members of the hinged four-link mechanism are set in the position I in such a way that the angle $B_1 A_1 C = 90^\circ$ and the angle $A_1 D B_1 = 0$. The flywheel 9 revolves autonomously at this time or is recharged with kinetic energy by the small-power motor 10 through the clutch 11. To set the flywheel 6 in motion, the clutches 5 and 8 are engaged and the clutch 11 is disengaged. The revolving flywheel 9 is now connected with the stationary flywheel 6 without any shock, because the transmission ratio from arm 1 to arm 2 is equal to $-\infty$. When the arm 1 turns from position I to position II through the angle $\psi_1 = 90^\circ$, the flywheel 6 is accelerated

by the flywheel 9 and the transmission ratio between the arms changes automatically from $-\infty$ to 0, which ensures a complete stop of the flywheel 9 in position II. Braking of the flywheel 6 and its stop in position III then occurs through the angle ψ_2 . The flywheel 9 is thereby accelerated to the maximum angular velocity. After this, the clutches 5 and 8 are disengaged. A turn of the arm 1 from position I to position III has thus been ensured while preserving a considerable part of the energy in the flywheel 9 which is left to rotate freely or, if required, to be recharged by the reversible motor 10. To ensure a turn of arm 1 into the original position, the clutches 5 and 8 are engaged, and the clutch 11 is disengaged. When the four-link mechanism passes into the position IV, the flywheel 6 is accelerated and the flywheel 9 is stopped in an angle of turn of the arm 1 of 90° and the flywheel 6 is then braked to a complete stop in an angle of turn of ψ_2 . After this, the mechanism returns to the original position. The energy losses for revolving the flywheel 6 are a result of its dissipation due to resistances in the drive. It is essential here that an accurate angle of turn ($\psi = \psi_1 + \psi_2$) of the arm 1 is ensured automatically by the ratio of the lengths of the members of the four-link mechanism; it depends on the dynamics of the turn only as regards the elasticity of the elements of the kinematic chain between the flywheels. When there is adequate rigidity, the increase of the mass (or of the moment of inertia) of the driven members of the manipulator and of the velocity of their motion does not affect the accuracy of the stop.

The principal characteristics of a manipulator will now be determined, using the recuperator. It will be assumed that during motion the moments of inertia of the moving members of the manipulator, reduced to the arm 1, are unchanged and equal to J_1 , and the moment of inertia of the flywheel 9, reduced to the arm 2, is equal to J_2 .

The equation of kinetostatic balance of the members 1 and 2 during an aerodynamic resistance to motion of the manipulator has the form

$$J_1 \ddot{\varphi}_1 + k \dot{\varphi}_1 + u J_2 \ddot{\varphi}_2 = 0. \quad (1)$$

Here and later on, $\varphi_1, \varphi_2, \dot{\varphi}_1, \dot{\varphi}_2, \ddot{\varphi}_1, \ddot{\varphi}_2$ are the angles of turn, counted from the direction CD (Fig. 1), the velocities and the accelerations of the members 1 and 2, respectively; $u = \dot{\varphi}_2 / \dot{\varphi}_1$ is the transmission ratio from arm 1 to arm 2 which depends on the angle φ_1 in conformity with known formulae, presented for example in Artobolevskii⁵; k is a coefficient of aerodynamic resistance.

The equation (1) can be transformed to a differential equation of the form

$$(i+u^2) \frac{d^2 \varphi_1}{d\varphi_1^2} + u u' \varphi_1 + a = 0,$$

Its solution will be, with due regard for the initial conditions (when $\varphi_1 = 0, \dot{\varphi}_1 = 0, \varphi_2 = \varphi_0$) the function

$$\varphi_1 = \frac{\varphi_0 - a \int_0^{\varphi_1} (i+u^2)^{-0.5} d\varphi_1}{\sqrt{i+u^2}}. \quad (2)$$

* Author's Claim No. 530132 (USSR).